$N(sp^3)$ to form an unconjugated ion with **11** and at $N(sp^2)$ atom to form a less well conjugated ion with **12**. On the other hand, **10** has the largest β value in Table I, i.e., this base (as well as other class I bases) has distinctly higher HBA basicity than most other known bases. This is accounted for by the relatively small dependence of HBA basicity on the valence-state electronegativities.

For inherently rather unstable bare ions, e.g., $CH_3C(=OH^+)H$ and NH_4^+,[19] bulk hydration energies are both large (~80 kcal/mol)[7] so that log $K_{b(aq)} \simeq$ log $K_{b(g)}$ for **1** and **4**. However, with increasing internal stabilization of BH^+ (as for all other bases of Table I), bulk hydration energies tend to become much smaller than for NH_4^+ so that log $K_{b(aq)}$ becomes much less than log $K_{b(g)}$. Indeed, for class I base **10**, the value of log $K_{b(aq)}$ is less than log $K_{b(g)}$ by a huge 28 units. Thus, an explanation has been provided for the basicity properties of class I compounds which were noted in the introductory statement. In support of this explanation, the following additional points may be made. There are no general correlations[20] between log $K_{b(aq)}$ values and the corresponding values of either log $K_{(g)}$ or $\Delta\beta$ of Table I. In spite of this, one finds *within a given family of bases* that if substituent polarizability effects are small or approximately constant there is the same sequence for all three kinds of basicity, e.g., **1 < 3 < 6 < 7 < 10**, **5 < 7**, **8 < 12**, and **9 < 11**. Also, if R, F, and P substituent effects are all relatively small or constant, the ξ order tends to emerge for all three basicity kinds, e.g., **6 < 8 < 9** and **1 < 2**.

In Table II eight basicity related properties are compared for the typical amide, *N,N*-dimethylacetamide, with the class I base R = C_2H_5 (or the very similar R_2 = c-$(CH_2)_5$. In all cases the class I base is shown to be distinctly stronger (which may be attributed largely to the much greater basicity of the "parent" base of the latter (**6**) compared with that of the former (**1**),- cf. Table I). All of the relevant properties of Table II are in excellent accord with the value of β = 1.06 for the class I base.[21] For example, the exothermicity of transfer of this base from the gas to dilute aqueous phase (26.6 kcal/mol) is the largest value yet reported for a neutral base (cf. Table 24 of ref 7). As expected for the conjugate acid of such a strong HBA base, the corresponding exothermicity of transfer of this HBD ion (60 kcal/mol) is the smallest value yet reported for a BH^+. This pair of observations is nicely consistent with the earlier observation that values of the difference log $K_{b(g)}$ - log $K_{b(aq)}$ are uniquely large for class I bases.

Acknowledgment. We are indebted to Professors C. Hansch and A. Leo for determination of the log $P_{o/w}$ value reported in Table II. We are also strongly indebted to Dr. R. Sabbah (C. T.M.-C.N.R.S., Marseille) for use of his calorimetric equipment and his help in obtaining the heat of vaporization (footnote *h* of Table II). Thanks also are due to Dr. J. P. Dubes (Université de Provence, Marseille) for checking the enthalpy of protonation in water (footnote *i* of Table II).

(19) The reader should appreciate that bare NH_4^+ is not the familiar form which is greatly stabilized by hydration or by ion aggregation. This may be appreciated by noting that log K_b values in Table I indicate that bare $NH_{4(g)}^+$ quantitatively protonates acetophenone whereas $NH_{4(aq)}^+$ quantitatively does not. We are indebted to a referee for suggesting clarification on this point.

(20) For log $K_{b(g)}$, values increase in the sequence **1-12**; for log $K_{b(aq)}$ the sequence is **1 < 5 < 3, 6 < 2 < 7 < 10 < 8 < 4 < 12 < 9 < 11**; for β values the sequence is **1 < 2, 4, 5 < 3 < 6 < 8 < 9 < 7, 11 < 12 < 10**.

(21) The gas-phase proton-transfer basicity of $[(CH_3)_2N]_3PO$ (whose β = 1.05 ± .01 also) has been reported[22] as log $K_{b(g)}$ = 17.7, which is 3.9 units less than that for **10**. This result is consistent with the lower ξ value for P=O, than, C=O (ref 3).

(22) Bollinger, J. C.; Houriet, R.; Yvernault, T. *Phosphorus Sulfur* **1984**, *19*, 379.

Vibrational Spectra and Assignments of $MeMn(CO)_5$ and $MeRe(CO)_5$ Species, Energy-Factored and A_1 Force Fields, and a Further Effect of Free Internal Rotation

G. P. McQuillan,* D. C. McKean, C. Long,[1a] A. R. Morrisson,[1b] and I. Torto

Contribution from the Chemistry Department, University of Aberdeen, Old Aberdeen AB9 2UE, Scotland. *Received March 22, 1985*

Abstract: The infrared spectra of $^{12}CH_3$, $^{13}CH_3$, $^{12}CD_3$, and $^{13}CD_3$ species of $MeMn(CO)_5$ and $MeRe(CO)_5$ have been studied in the gas phase to 450 cm^{-1} and in the solid at 78 K down to 200 cm^{-1}. Solid-phase Raman spectra (600-300 cm^{-1}) for $MeRe(CO)_5$ are also reported. Nearly all of the δ(MCO) and ν(MC) modes are assigned with confidence in both compounds, and two reassignments are proposed for $MeMn(CO)_5$. An energy-factored force field is calculated for the CO stretching vibrations by using gas-phase data which include the B_1 fundamental. An A_1 force field for all vibrations shows that all the metal-carbon bonds increase in strength from Mn to Re, while the methyl CH bond is weakened. The axial and equatorial M-CO bonds in $MeRe(CO)_5$ are equal in strength, suggesting a negligible trans effect on the part of the methyl ligand. This is interpreted in terms of equal and opposite π- and σ-trans effects, the former strengthening the axial Re-CO bond and the latter weakening it. The gas-phase contour of the absorption complex assigned to $\rho(CH_3)$ in $MeRe(CO)_5$ resembles those due to $\nu_{as}(CH_3)$ and $\nu_{as}(CD_3)$ and is attributed to a variation in the rocking force constant with internal rotation angle, together with free internal rotation. The corresponding band in $MeMn(CO)_5$ may also reflect the same effect.

In a previous paper[2] we discussed the infrared spectra of $^{12}CH_3$, $^{13}CH_3$, $^{12}CD_3$, $^{13}CD_3$, and CHD_2 labeled species of $MeMn(CO)_5$ and $MeRe(CO)_5$ in the CH and CD stretching frequency regions, with reference to the effects of free internal rotation on these bands in the gas phase. In this work we report new infrared gas- and solid-phase data for $MeMn(CO)_5$ species, which complement the extended study recently published by Andrews et al.[3] and assign vibrations in the 700-300-cm^{-1} region, leaning heavily on previous work and on similar studies of $BrMn(CO)_5$[4] and $M(CO)_6$ (M =

(1) (a) Present address: National Institute for Higher Education, Dublin 9, Ireland. (b) Present address: R.G.I.T., St. Andrew Street, Aberdeen, Scotland.

(2) Long, C.; Morrisson, A. R.; McKean, D. C.; McQuillan, G. P. *J. Am. Chem. Soc.* **1984**, *106*, 7418.

(3) Andrews, M. A.; Eckert, J.; Goldstone, J. A.; Passell, L.; Swanson, B. *J. Am. Chem. Soc.* **1983**, *105*, 2262.

(4) Ottesen, D. K.; Gray, H. B.; Jones, L. H.; Goldblatt, M. *Inorg. Chem.* **1973**, *12*, 1051.

0002-7863/86/1508-0863$01.50/0

Table I. Infrared Frequencies in the Gas Phase, 2200–1800 cm^{-1}, of the $MeMn(CO)_5$ Species[a,d]

$^{12}CH_3$	$^{13}CH_3$	$^{12}CD_3$	$^{13}CD_3$	assignment
2147.2 sh		2147.4 sh	2147.0 sh	2024 + 121
2142.2 sh		2141.1 sh	2140.9 sh	2044 + 90
2133.8 sh		2133.3 sh	2134 sh	2024 + 110
2116.5 q, m	2116.6 m	2113.0 m	2111.2 m	$\nu_2(A_1)$ $\nu(CO^{eq})$
2097 sh				2024 + 80
2083.4 q, vw		*b*	2082.7 sh	2004 + 81
2043.9 sh		2043.4 sh	2043 sh	$\nu_{12}(B_1)$ $\nu(CO^{eq})$
2024.4 q, vs		2024.0 vs		$\nu_{19}(E)$ $\nu(CO^{eq})$
2003.6 q, vs	2003.4 vs	2003.5 vs	2003.3 vs	$\nu_3(A_1)$ $\nu(CO^{ax})$
1988.5 q, sh		1988.3 q, sh		$\nu(^3CO^{eq})$
1961.8 q, w		1961.9 w	1961.7 w	$\nu(^{13}CO^{ax})$
1944.8 vvw		1945.4 ww	1945.1 vvw	2024–80
1922.7 q, vw		1922.8 vw	1922.9 vw	2004–81 2024–102
1903.5 sh			~1904 sh	2004–100 2024–121
	1860 xw		1867.8 xw	2004–144, 136

[a] For ν(CH) and ν(CD) frequencies, see ref 2. Nonfundamental bands above 2200 cm^{-1} are listed in Supplementary Table I, with suggested assignments. [b] Obscured by the ν(CD) band. [c] Narrow Q branch, often accompanied by P and R branches, not separately listed. [d] v = very, x = extremely.

Cr, Mo, W) compounds.[5] We report similar infrared and some Raman solid-state data for $MeRe(CO)_5$ species, with consequent assignments. The rhenium compound has been much less studied[6,7] than $MeMn(CO)_5$ and in particular there are no previous assignments of the MC stretching modes. These were of special interest as we wished to compare metal–methyl stretching force constants in the Mn and Re compounds to see if the decrease in $\nu(CH^{is})$ established in our earlier study,[2,8] from Mn to Re, was accompanied by an increase in metal–CH_3 bond strength, an inverse relationship which we have observed elsewhere in group II and group IV compounds.[9] A bonus from the gas-phase spectra was the observation, in both compounds, of all four CO stretching fundamental bands, and of further effects ascribed to free internal rotation of the methyl group. The ν(CO) data provide the basis for complete energy-factored force fields, to be compared with a recent one for $MeMn(CO)_5$ based on matrix-isolation frequency data,[10] and the $\nu(CH_3)$ spectra in the gas phase provide further evidence that the conclusions concerning internal rotation of Dempster et al.,[11] who also reported gas-phase spectra of $CH_3Mn(CO)_5$ and $CD_3Mn(CO)_5$, are incorrect.

Experimental Section

The compounds were prepared from appropriately labeled methyl iodides, as described previously.[2] Infrared spectra in the gas phase were obtained with a Nicolet 7199 FTIR spectrometer employing ordinary and multiple-reflection cells with path lengths up to 8 m, at resolutions of 0.25 or 0.5 cm^{-1}. Infrared solid-phase spectra were obtained from films deposited from the vapor on a CsI window cooled to 78 K, using a Perkin-Elmer 225 spectrometer with resolution of about 1 cm^{-1}. Frequency accuracy varied from ±0.1 cm^{-1} (±0.2 cm^{-1} for ^{12}C–^{13}C shifts) for bands in the gas phase having well-developed PQR contours to ±1 cm^{-1} (0.5–1.0 cm^{-1} for ^{13}C shifts) for bands in the solid phase. In general the films, which were not specially annealed, were highly transparent, allowing measurements to be made on very weak bands.

Raman spectra for the $MeRe(CO)_5$ species were obtained at room temperature on a Cary 83 Raman spectrometer with argon-ion laser excitation (488.0 nm, ca. 50 mw at sample). The spectra were recorded at room temperature for crystalline samples in sealed capillaries; the spectrometer was fitted with an external recorder and calibrated with appropriate neon emission lines in a continuous run with the sample spectrum. Frequency accuracy here is about ±1 cm^{-1}, with several ^{12}C–^{13}C shifts perhaps good to ±0.5 cm^{-1}. In some samples there was evidence of a small amount of impurity in the form of a weak sharp line, of variable intensity, near 350 cm^{-1}; a number of the gas-phase spectra of $MeRe(CO)_5$ also contained a very weak band, with Q branch sequence commencing at 806.8 cm^{-1}, which must have arisen from a light impurity molecule with quite different size and shape from that of the rhenium compound.

Detailed Raman frequency data for $MeMn(CO)_5$ are available from the work of Andrews et al.[3]

Table II. Infrared Frequencies in the Gas Phase, 2200–1800 cm^{-1}, in the $MeRe(CO)_5$ Species[a]

CH_3[b]	CD_3[b]	assignment
2132.8 q, m (0)	*c*	$\nu_2(A_1)\nu(CO^{eq})$
2109.9 q, wm (0)	2109.8 q, wm (?)	2026 + 84
2076.2 q, w (0)	2075.5 q, w (?)	1998 + 76
2050.8 q, wm (0) 2041.3 sh	2050.8 q, wm (0)	$\nu_{12}(B_1)\nu(CO^{eq})$ and 2133 − 82 or 92
2025.9 q, vs (0)	n.o.[e]	$\nu_{19}(E)\nu(CO^{eq})$
1997.6 q, vs (0)	n.o.[e]	$\nu_3(A_1)\nu(CO^{ax})$
1955.3 q, m (0)	1955.3 q, m (0)	$\nu(^{13}CO^{ax})$
1921.8 q, w (0)	1922 w (0)	1998–76
1869 vw (0)	1878 vw, bd (0)	1998–129 (ν_{26}, E)

[a] For ν(CH) and ν(CD) frequencies, see ref 2. Nonfundamental bands above 2200 cm^{-1} are listed in Supplementary Table II with suggested assignments. [b] In brackets, ^{12}C–^{13}C shifts. [c] Obscured by ν(CD) bands. [d] Narrow Q branch, often accompanied by P and R branches, not separately listed. [e] Not observed.

Table III. Carbonyl Stretching Force Constants for $MeM(CO)_5$ in the Gas Phase[d]

	M = Mn		M = Re	
	obsd	calcd	obsd/ calcd(1)	obsd/ calcd(2)
A_1	2116.5	2116.5	2132.8	2132.8
B_1	2043.9	2043.9	2051.0	2041.3
E	2024.4	2024.3	2025.9	2025.9
A_1	2003.6	2003.4	1997.6	1997.6
$^{13}CO^{eq}$	1988.5	1988.7	(1990.2)	(1989.2)
$^{13}CO^{ax}$	1961.8	1640.2	1955.3	1955.3
$f_{CO^{ax}}$	16.402	(16.278)[a]	16.270	16.270
$f_{CO^{eq}}$	16.971	(16.821)[a]	17.097	17.053
$\lvert f_{CO^{ax}CO^{eq}}\rvert$[b]	0.283	(0.218)[a]	0.283	0.283
$f_{CO^{eq}CO^{eq}}{}^{cis}$	0.258	(0.369)[a]	0.308	0.348
$f_{CO^{eq}CO^{eq}}{}^{trans}$	0.418	(0.453)[a]	0.514	0.474
$F_{CO^{eq}}(A_1)$[c]	17.905		18.227	18.227

[a] Values determined in CH_4 matrix at 12 K.[10] [b] The sign is indeterminate since the G matrix is diagonal and there is no information about the composition of the A_1 normal coordinates. The two solutions for a 2 × 2 problem can then differ only in the size of the off-diagonal constant. [c] Symmetry force constant = $F_{7,7}$ in Table VI. [d] Units: mdyn/Å.

Results and Discussion

Carbonyl Stretching Region: $MeMn(CO)_5$ and $MeRe(CO)_5$. Frequencies for the region 2800–1800 cm^{-1} are listed in Tables I and II. Figure 1 shows some infrared spectra at varying path lengths for $^{12}CH_3Mn(CO)_5$ in the gas phase. A similar diagram for the rhenium compound appeared in Figure 9 of ref 2.

The spherical top type contours of the main bands are very evident. The Q branch of the very intense *E* species fundamental at 2024.4 cm^{-1} (Mn) or 2025.9 cm^{-1} (Re) is slightly broader than that of the strong A_1 band at 2003.6 cm^{-1} (Mn) or 1997.6 cm^{-1} (Re), which could arise from a very small lifting of the degeneracy or from other sources. Weaker peaks at 1988.5 and 1961.8 cm^{-1} (Mn) and 1955.3 cm^{-1} (Re) are readily identified as due to natural abundance $^{13}CO^{eq}$ and $^{13}CO^{ax}$ species (the band due to the former in the rhenium compound is calculated to be too close to $\nu_3(A_1)$

(5) Jones, L. H.; McDowell, R. S.; Goldblatt, M. *Inorg. Chem.* **1969**, *8*, 2349.
(6) Hieber, W.; Braun, G.; Beck, W. *Chem. Ber.* **1960**, *93*, 901.
(7) Wilford, J. B.; Stone, F. G. A. *Inorg. Chem.* **1965**, *4*, 389.
(8) $\nu(CH^{is})$ is defined as the isolated CH stretching frequency observed in the CHD_2-substituted methyl species.
(9) McKean, D. C.; McQuillan, G. P.; Thompson, D. *Spectrochim. Acta* **1980**, *36A*, 1009.
(10) McHugh, T. M.; Rest, A. J. *J. Chem. Soc., Dalton Trans.* **1980**, 2323.
(11) Dempster, A. B.; Powell, D. B.; Sheppard, N. *J. Chem. Soc. A* **1970**, 1129.
(12) Hitam, R. B.; Narayanaswamy, R.; Rest, A. J. *J. Chem. Soc., Dalton Trans.* **1983**, 615.

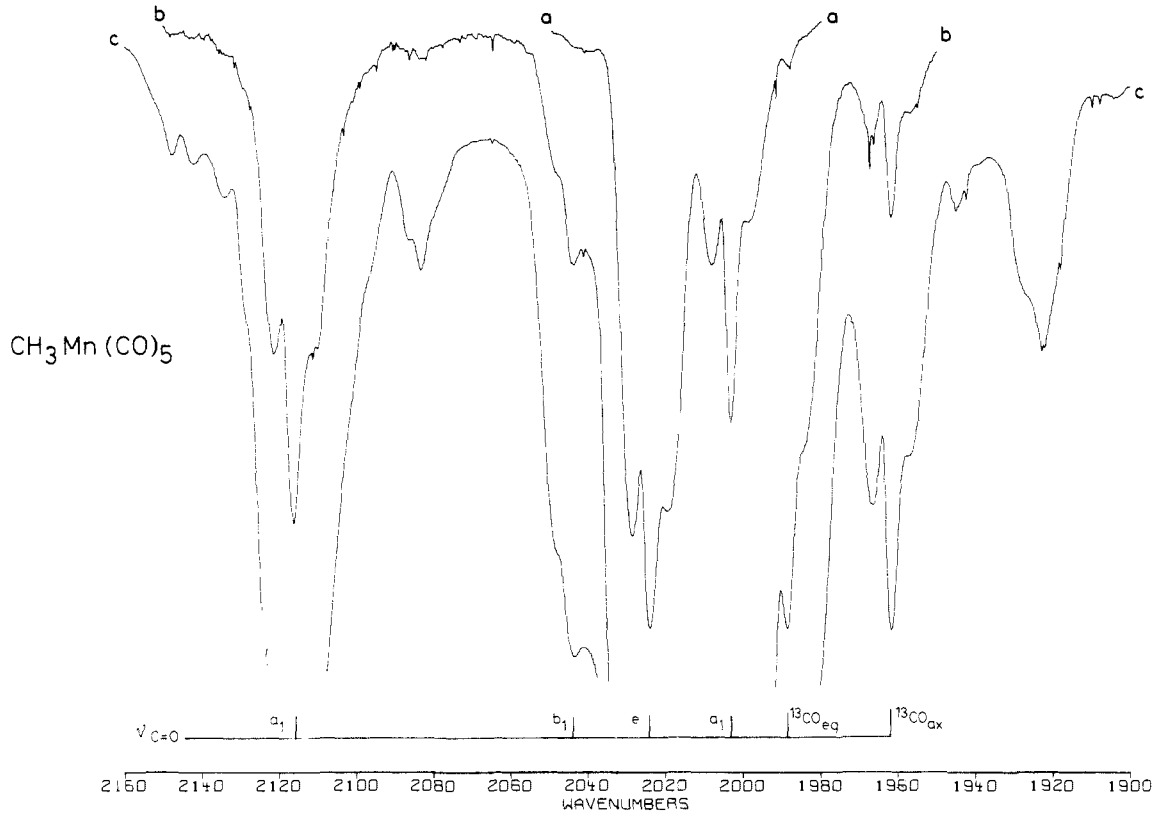

Figure 1. Infrared spectrum in gas phase of $^{12}CH_3Mn(CO)_5$: (a) 5 torr in 10 cm, resolution 0.12 cm^{-1}; (b) 2 torr in 75 cm, resolution 0.12 cm^{-1}; (c) 4 torr in 2.3 m, resolution 0.5 cm^{-1}.

to be measurable). This information then allows all five constants of the energy-factored force field to be calculated for the Mn compound, as seen in Table III, from which the B_1 fundamental could be identified as the weak band at 2043.9 cm^{-1}. All six frequencies can in fact be fitted by the five-parameter function to within ±0.2 cm^{-1}, as seen in Table III, which is another example of the remarkable, if fortuitous success of this type of calculation.[13,14] The interaction constants from the gas-phase data differ slightly from those previously determined in a CH_4 matrix at 12 K.[10] This might be an illusion deriving from changes in anharmonicity. While the sign of $f_{CO^{ax}\text{-}CO^{eq}}$ is inevitably indeterminate, it would be physically unrealistic to suppose it to be negative.

Only one ^{13}CO band is visible in the $MeRe(CO)_5$ spectrum, so no exact prediction of the B_1 fundamental is possible. There are two weak bands near where it would be expected, at 2050.8 and 2041.3 cm^{-1}, respectively. When these are used in turn to calculate all five parameters, the sets of constants (1) and (2) in Table III are obtained. These differ only slightly from each other, but both differ significantly from the Mn constants, in that the axial constant $f_{CO^{ax}}$ falls from Mn to Re, while the equatorial constant $f_{CO^{eq}}$ rises slightly. There are also changes in the interaction constants such that the A_1 equatorial symmetry constant rises appreciably from Mn to Re, by 0.32 mdyn $Å^{-1}$. This rise, however, is not reproduced in the A_1 force field (below). One of the two bands at 2050.8 and 2041.3 cm^{-1} is presumably a difference band involving the A_1 2132.8-cm^{-1} fundamental and a skeletal frequency of 82 or 92 cm^{-1}. In so far as the bands at 2109.9 and 2216.8 cm^{-1} can be assigned as combinations involving a frequency of 84 cm^{-1}, the evidence slightly favors the choice of 2041.3 cm^{-1} as $\nu_{12}(B_1)$. Finally, the force fields (1) and (2) for the Re compound both predict the $^{13}CO^{eq}$ band close to 1990 cm^{-1}: the proximity of this band to the A_1 fundamental accounts for our inability to observe it.

CH_3 Deformation and Rocking bands. Frequencies below 1500 cm^{-1} are listed in Tables IV and V. Figure 2 shows the infrared spectrum of $^{13}CH_3Re(CO)_5$ in the gas phase. Absorption in the neighborhood of 1400 cm^{-1} in the gas-phase spectra of $CH_3Mn(CO)_5$ and $CH_3Re(CO)_5$ is weak and so indefinite that it would be unsafe to attempt to distinguish $\delta_{as}(CH_3)$ from neighboring combination bands. However, in the solid film at 78 K more definite bands are seen, at 1419 (Mn) and 1429 cm^{-1} (Re), with ^{13}C shifts of about 3 cm^{-1} which confirm their origin as $\delta_{as}(CH_3)$ transitions. In the CD_3 compounds bands near 1039 cm^{-1} in both phases appear to be due to $\delta_{as}(CD_3)$.

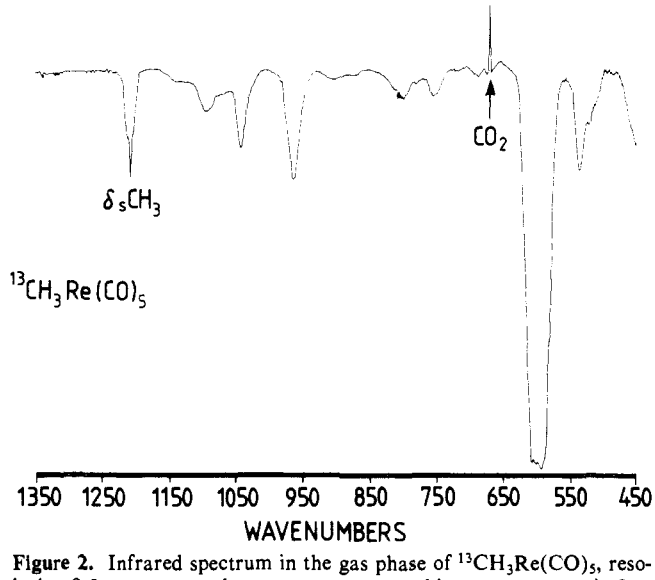

Figure 2. Infrared spectrum in the gas phase of $^{13}CH_3Re(CO)_5$, resolution 0.5 cm, saturated vapor pressure at ambient temperature in 8 m cell. Atmospheric CO_2 and an unidentified impurity produce bands at 667 and ~807 cm^{-1}, respectively. See ref 11 for a spectrum of $CH_3Mn(CO)_5$ in this region.

The symmetric deformation bands are observed at 1191.1 (Mn) and 1212.0 cm^{-1} (Re), each with a narrow central maximum and incipient P and R branches, allowing accurate ^{13}C shifts to be determined. It is interesting here that the $\delta_{as}(CH_3)$ and $\delta_s(CH_3)$

(13) Perutz, R. N.; Turner, J. J. *Inorg. Chem.* **1975**, *14*, 262.
(14) Jones, L. H. *Inorg. Chem.* **1976**, *15*, 1244. Burdett, J. K.; Perutz, R. N.; Poliakoff, M.; Turner, J. J. *Inorg. Chem.* **1976**, *15*, 1245.

Table IV. Infrared Frequencies of $MeMn(CO)_5$ Species, 1500–300 cm^{-1} [a]

CH_3[b]		CD_3[b]		
gas[f]	solid[c]	gas[f]	solid[c]	assignment
	1432 sh, bd			
	1419 w (3.0)			ν_{20}, E, $\delta_{as}(CH_3)$
1191.1 m (5.1)	1176 s (4.8)			ν_4, A_1, $\delta_s(CH_3)$
		1039.5 w (0)	1036 w (2)	ν_{20}, E, $\delta_{as}(CD_3)$
		903.1 q, m (8.2)	892 m	ν_4, A_1, $\delta_s(CD_3)$
869 vw (0)	880 w (0)	867 w (0)		500 + 374?[d]
858 vw (0)	867 w (0.5)	858 w (0)	865 sh, bd	492 + 374
834 vw (0)	836 w (0)	832 sh (0)	835 vw (0)	458 + 374
			800 sh (0)	
~755 bd as, vw (0)	784.5 m (2.8)			ν_{21}, E, $\rho(CH_3)$
			760 vw (1)	664 + 100 ?
668 sh				ν_5, A_1, $\delta(MCO^{eq,op})$
655.4 vs (0)	645 vvs, as, bd	666.9 vs (0.3)	655 vvs, as, bd	ν_{22}, E, $\delta(MCO^{eq,ip})$
603 sh (0)	~612? sh (0)			ν_{13}, B_1, $\delta(MCO^{eq,op})$?[d]
		599.5 m (2.1)	584.5 (2)	ν_{21}, E, $\rho(CD_3)$
571 sh (3)	558 sh		556 vw (0)	ν_{16}, B_2, $\delta(MCO^{eq,ip})$?[d]
558.0 w (0.9)	553 w (0)	548.4 w (0.4)	543 wm (1)	ν_{23}, E, $\delta(MCO^{ax})$
(499 sh)	505 sh (0)	500 sh (0)	504 vw (0)	$\nu_8 + \nu_9$?[d,e]
491.9 m (5)	496 w (3.5)	~481 m (2?)	491 w (2)	ν_6, A_1, $\nu(M-CO^{ax})$[g]
484 sh (0)				
~458 s (~0)	463 vs (0)	~456 s (458)	462 vs (0)	ν_{24}, E, $\nu(M-CO^{eq})$
438.5 sh (1.2)	439.7 wm (0.6)	(436.1)	437.7 wm (0)	ν_{25}, E, $\delta(MCO^{eq,op})$
n.o.	(422.5)	n.o.	423 vw (0)	ν_{14}, B_1, $\nu(M-CO^{eq})$
n.o.	(418.5)	n.o.	419 sh (0)	
n.o.	420 w (9.0)	n.o.	400 w (8.0)	ν_7, A_1, $\nu(M-CH_3)$[g]
n.o.	405 w (0)	n.o.	408 sh (0)	ν_8, A_1, $\nu(M-CO^{eq})$[g]
n.o.	374 vw (0)	n.o.	374 vw (0)	ν_{10}, A_2, $\delta(MCO^{eq,ip})$

[a] Nonfundamental bands between 1500 and 900 cm^{-1} are listed in Supplementary Table III, with suggested assigments. [b] In brackets, $^{12}C-^{13}C$ shifts, or ^{13}C frequencies. [c] At 78 K. [d] Provisional assignments, see text. [e] ν_9, δ(CMC), A_1, ref 3. [f] n.o. = not observed. [g] See also Table VIII.

Table V. Vibrational Frequencies of $MeRe(CO)_5$ Species, 1500–350 cm^{-1} [a]

CH_3[b]			CD_3[b]			
IR gas[e]	IR solid[c]	R solid	IR gas[e]	IR solid	R solid	assignment
	1428.6 wm (3.1)					ν_{20}, E, $\delta_{as}(CH_3)$
1212.0 q, w (5.7)	1193 m (5)					ν_4, A_1, $\delta_s(CH_3)$
				1054 w (0)		
			1039 w (0)	1037 sh		ν_{20}, E, $\delta_{as}(CD_3)$
			923.4 q, vw (9.3)	910.2 w (10.0)	~911 m (~8)	ν_4, A_1, $\delta_s(CD_3)$
802 vw (~5)						
783 xw (4)	777.5 w (4)					ν_{21}, E, $\rho(CH_3)$
758 vw (~5)						
727 xw (0)			728 xw			
687 vw (0)			690 xw			609 + 76
673 sh						595 + 76
609.1 q, vs (0.5)	603.2 vs, as (0)		607.5 vs	600.2 vs, as		ν_5, A_1, $\delta(MCO^{eq,op})$
595.5 vs (0.3)	586.0 vs, as (~0)					ν_{22}, E, $\delta(MCO^{eq,ip})$
				(589 vw, sp)		ν_{13}, B_1, $\delta(MCO^{eq,op})$[d]
			585 s	577 vw, as (0)		ν_{21}, E, $\rho(CD_3)$
535 w (1)	532.6 m (1.1)	~531 w, bd	531 sh (2)	~533 sh (0)	531 vw	ν_{16}, B_2, $\delta(MCO^{eq,ip})$[d]
522 sh (2)			516 m (0)	522 m (0)		ν_{23}, E, $\delta(MCO^{ax})$
	502.5 vw (0)	~508 w, bd		502.6 vw (0)	502 sh	Comb?[d]
462 sh	472.7 vw (5.2)	471.3 vs (4.7)		464.0 w (0.8)	463 vs (1.4)	ν_6, A_1, $\nu(M-CO^{ax})$[f]
(444 sh)	454.5 m (2.0)	~450 sh	~444 m (0)	451.0 m (0)	~448 sh	ν_8, A_1, $\nu(M-CO^{eq})$[f]
	447 sh (?)	450.1 s (6.1)			425.6 s (9.1)	ν_7, A_1, $\nu(M-CH_3)$[f]
(435 m)	434.2 w (0)		432 sh (0)	431.1 w (0)	~431 sh	ν_{25}, E, $\delta(MCO^{eq,op})$
n.o.	418 xw?		n.o.	418 xw?		ν_{14}, B_1, $\nu(M-CO^{eq}?)$[d]
n.o.	375 vs, as	~380 w, bd	n.o.	375 vs, as (0)	~379 w, bd	ν_{24}, E, $\nu(M-CO^{eq})$[g]

[a] Nonfundamental bands between 1500 and 800 cm^{-1} are listed in Supplementary Table IV, with suggested assignments. [b] In brackets, $^{12}C-^{13}C$ shifts. [c] At 78 K. [d] Provisional assignments, see text. [e] n.o. = not observed. [f] See also Table VIII. [g] Obscures ν_{10}?

modes are both higher in the rhenium compound than in the manganese compound. This may reflect the decrease in HCH angle from 108.0 (Mn) to 107.1° (Re) predicted from $\nu(CH^{is})$ data for the $CHD_2M(CO)_5$ species.[2]

The band at 755 cm^{-1} in the gas-phase spectrum of $CH_3Mn(CO)_5$ has long been assigned to $\rho(CH_3)$, moving to 600 cm^{-1} on deuteration,[3,11] where it displaces upward the intense band due to ν_{22}(E) (δ(MCO)) near 660 cm^{-1}.[3] The ^{13}C shift on the 755-cm^{-1} band is indeterminate because of a change in shape, but there is a striking *upward* shift of about 30 cm^{-1} on passing to the solid phase. This is unusual in itself and even more so in contrast with $\rho(CD_3)$, which *falls* by about 16 cm^{-1} on condensation.

In the rhenium compound there is a conspicuous solid-phase band at 777.5 cm^{-1} which since it disappears on deuteration and has a ^{13}C shift of 4 cm^{-1} is clearly due to $\rho(CH_3)$. The corresponding $\rho(CD_3)$ band is at 577 cm^{-1}. In the gas phase, however (Figure 3), two very weak broad maxima, at 802 and 758 cm^{-1}, together with a weaker sharp peak at 783 cm^{-1}, all appear to exhibit a ^{13}C shift of about 4 cm^{-1} and to disappear on deuteration. As in the Mn compound, the lowest peak, at 758 cm^{-1}, lies substantially below the solitary solid frequency. The overall appearance and behavior of the $\rho(CH_3)$ band is such as to mimic that of the $\nu_{as}(CH_3)$ and $\nu_{as}(CD_3)$ bands, which we attributed in our previous paper[2] to the effect of free internal rotation of the

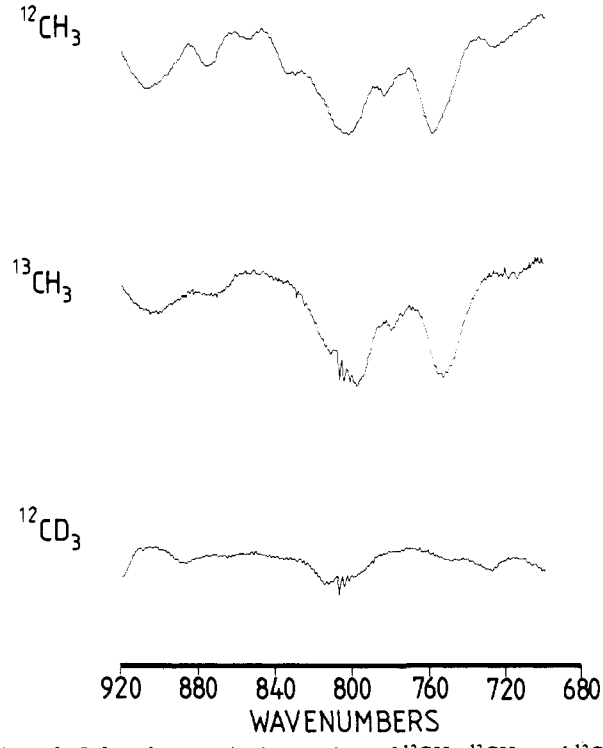

Figure 3. Infrared spectra in the gas phase of $^{12}CH_3$, $^{13}CH_3$, and $^{12}CD_3$ species of $MeRe(CO)_5$, in the $\rho(CH_3)$ region; conditions as in Figure 2. The 807-cm^{-1} impurity band is isolated and more intense in the $^{12}CD_3$ spectrum.

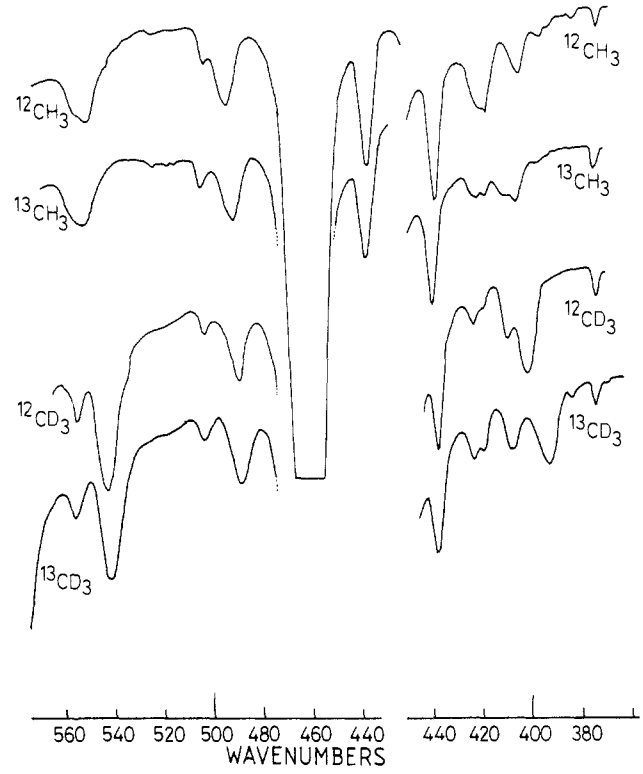

Figure 4. Infrared spectrm of the $MeMn(CO)_5$ species in solid films at 78 K (Perkin-Elmer 225 spectrometer, resolution ~1 cm^{-1}).

methyl group combined with a force constant variation occurring during the rotational motion. By analogy with the Sheppard and Woodman treatment[15] of a CH_3XY_2 system this leads to the splitting of a normally degenerate band. It is clear from the above treatment that the source of the force constant variation needed to generate the effect is irrelevant. In the present instance we would require only that rocking in the direction of one of the planes of symmetry involved a different change of potential energy from motion at 45° to such planes. The appearance of the weak central maximum at 783 cm^{-1} in the gaseous rhenium compound, slightly above the midpoint of the two outer bands just as in the $\nu_{as}(CH_3)$ and $\nu_{as}(CD_3)$ bands,[2] is particularly suggestive of a force constant variation effect. The doublet spacing, 802 − 758 = 44 cm^{-1}, is, however, significantly less than in the $\nu_{as}(CH_3)$ spectrum (68 cm^{-1}) which could reflect a smaller variation in force constant.

A merit of this interpretation is that there is then a small *downward* shift in frequency from the center of gravity of the gas-phase complex to the solitary solid-phase frequency, which is more acceptable on empirical grounds.[16]

There is no sign of any comparable splitting in the broad $\rho(CD_3)$ band at 585 cm^{-1}, although this is partly overlapped by the intense band due to $\nu_{22}(E)$. The absence of internal rotation effects comparable to those suggested for $\rho(CH_3)$ is readily explained by the extensive coupling between $\delta(MCO)$ and $\rho(CD_3)$ motions which must be present.

If we adopt the foregoing interpretation for $\rho(CH_3)$ of $CH_3Re(CO)_5$, then a similar effect would be expected in $MeMn(CO)_5$, where, however, only one band is seen in the 800-cm^{-1} region. The startling rise in frequency (30 cm^{-1}) of this band on passing from the gas to the solid phase emboldens us to suggest that here too we may have a situation of free internal rotation with force constant variation but that the transition moment in one of the unique directions is very much less than that in the other, so that only one component of the doublet has significant intensity.

A final reflection here is that the difficulty of identifying $\delta_{as}(CH_3)$ bands in the gas-phase spectra may well arise from similar free internal rotation/force constant variation effects, causing the bands to broaden or split into several components, not necessarily all of comparable intensity.

Region 700–300 cm^{-1}: $MeMn(CO)_5$. With two exceptions, the bands listed in Table IV all have counterparts in the earlier IR and Raman spectra.[3] We observe *two* frequencies near 420 cm^{-1} in the infrared spectra of solid films of the $^{13}CH_3$, $^{12}CD_3$, and $^{13}CD_3$ species (Figure 4) [in the $^{12}CH_3$ species, these would be obscured by the band due to $\nu_7(A_1)$ ($\nu(M-CH_3)$)] and in the same phase, in all four species, a very weak band at 374 cm^{-1}. There are thus two more frequencies than there are fundamentals to account for them, the latter including five $\nu(MC)$ and seven $\delta(MCO)$ modes (see Table I of ref 3). There can be little doubt about eight of these fundamentals. $\nu_5(A_1)$ ($\delta(MCO^{eq,op})$) is visible as a shoulder near 668 cm^{-1} in the vapor spectrum of the $^{12}CH_3$ species, above the intense band due to $\nu_{22}(E)$ ($\delta(MCO^{eq,ip})$) the latter displaced upward by $\rho(CD_3)$ as identified earlier.[3] The three A_1 $\nu(MC)$ modes were readily assigned through their $^{12}C-^{13}C$ shifts in the infrared solid spectra, even before the Raman evidence became available[3] to confirm the crossing over of ν_7 ($\nu(M-Me)$) and ν_8 ($\nu(M-CO^{eq})$) on deuteration. The very intense infrared band in the solid at 463 cm^{-1} must surely arise from the E species $\nu(M-CO^{eq})$ mode ν_{24}, while the weak bands at 553 and 439 cm^{-1}, which both exhibit deuteration shifts, the latter admittedly small, must derive from the E species $\delta(MCO)$ modes ν_{23} and ν_{25}, also in agreement with ref 3.

Three $\delta(MCO)$ modes, $\nu_{10}(A_2)$, $\nu_{13}(B_1)$, and $\nu_{16}(B_2)$, remain to be assigned, plus the last $\nu(MC)$ mode, $\nu_{14}(B_1)$, with six frequencies still unaccounted for at 603 (g), 558 (s), ~500 (g, s), 423 (s), 419 (s), and 374 (s) cm^{-1}, all with no detectable isotopic frequency shifts. An obvious assignment for the 374-cm^{-1} band is the lowest $\delta(MCO)$ mode, $\nu_{10}(A_2)$, deriving as it does from the F_{1g} frequency ν_5 in octahedral $M(CO)_6$, which is found at 368 cm^{-1} in solid $Cr(CO)_6$.[5] The B_1 and B_2 $\delta(MCO)$ modes derive

(15) Sheppard, N.; Woodman, C. M. *Proc. R. Soc. London* **1969**, *A313*, 149.

(16) While it is true that an exact Fermi resonance with an overtone level such as 2 × 375 cm^{-1} could also produce the two bands and a normal gas–solid shift, the resulting ^{13}C shift of ~8 cm^{-1} in the unperturbed $\rho(CH_3)$ band would be unacceptably high.

(17) A change in contour on ^{13}C substitution makes it hard to determine a meaningful $^{12}C-^{13}C$ frequency shift in the gas phase.

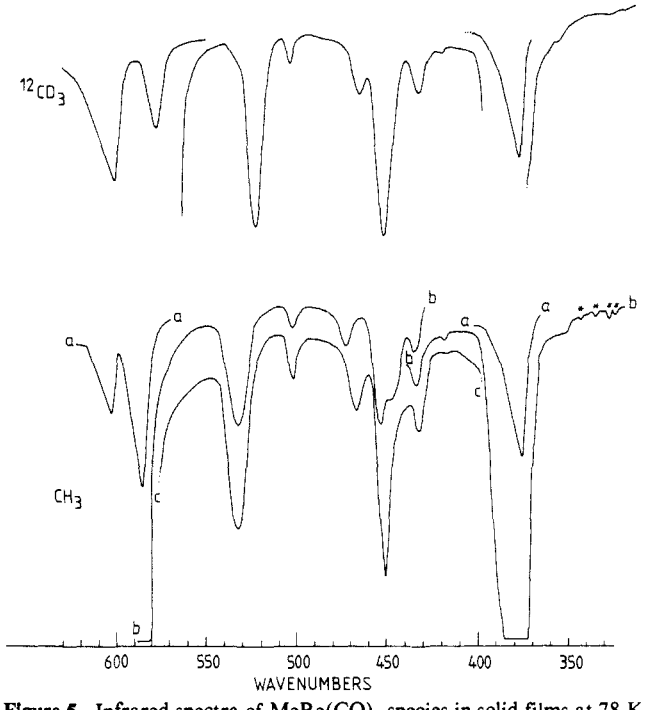

Figure 5. Infrared spectra of $MeRe(CO)_5$ species in solid films at 78 K (conditions as for Figure 4): (a, b) $^{12}CH_3$ species, (c) $^{13}CH_3$; (*) atm. H_2O.

respectively from the F_{2g} and F_{2u} modes of $M(CO)_6$, both of which occur above 500 cm^{-1} in the chromium compound. Combinations with skeletal modes between 80 and 180 cm^{-1} are more likely to account for extra bands above 450 cm^{-1} than below it. Therefore we think that the solid band at 423 cm^{-1} is due to the ν(MC) mode $\nu_{14}(B_1)$ leaving the shoulder at 419 cm^{-1} unexplained.

Our assignments differ from those of Andrews et al.[3] with respect to ν_{10} (374 instead of 423 cm^{-1}) and ν_{14} (423 instead of 506 cm^{-1}). The last two δ(MCO) modes, $\nu_{13}(B_1)$ and $\nu_{16}(B_2)$, remain problematical, with three frequencies available (603, 558, and ~500 cm^{-1}). If the earlier assignments[3] of ν_{13}, ~600 cm^{-1}, and ν_{16}, 560 cm^{-1}, are accepted, the band at ~500 cm^{-1} has to be a combination, for which $\nu_8(A_1) + \nu_9(A_1)$ is an obvious choice. This assignment seems to be broadly compatible with the spectrum of the rhenium compound (see below). However, a fundamental at ~500 cm^{-1} would give the best explanation of the combination at 941 cm^{-1}, and combinations between 850 and 800 cm^{-1} also seem to be more readily assignable on the basis of fundamentals at ~500 and 374 cm^{-1}.

The probable difference bands between 1945 and 1860 cm^{-1} raise possibilities for skeletal fundamentals at 80, 100, 121, or 144 cm^{-1}. The 8-cm^{-1} upward deuteration shift in the 1860-cm^{-1} band suggests that this arises from ν_{26}(E) at 144 cm^{-1} in the gas phase, which is reported in solution at 153 cm^{-1} with a shift of 11 cm^{-1}.[13] A band at 2670 cm^{-1}, with no significant deuteration or ^{12}C–^{13}C shift, corresponds to the combination (2117 + 558) cm^{-1} and provides additional evidence for an isotope-independent fundamental at the latter frequency.

Region 700–300 cm^{-1}: $MeRe(CO)_5$. Figure 5 shows the solid film infrared spectra of $MeRe(CO)_5$ species.

Examination of the trends in the fundamentals of $M(CO)_6$ compounds (M = Cr, Mo, W)[5] shows that we might expect the following changes in δ(MCO) frequencies from $MeMn(CO)_5$ to $MeRe(CO)_5$: $\Delta\nu_5(A_1)$(eq,op) ~ −80 cm^{-1}, $\Delta\nu_{13}(B_1)$(eq,op) ~ +10 cm^{-1}, $\Delta\nu_{16}(B_2)$(eq,ip) ~ −50 cm^{-1}, and $\Delta\nu_{10}(A_2)$(eq,ip) ~ 0 cm^{-1}, the high figure for ν_5 deriving in part from the change in mass of the moving metal atom. Trends in the E modes are harder to predict, but the highest of these, ν_{22}(eq,ip), which also involves substantial movement of the metal atom, should also exhibit a marked downward shift.

In fact ν_5 and ν_{22} both move down by about 60 cm^{-1} and are seen clearly resolved in the gas phase at 609.1 and 595.5 cm^{-1} in $CH_3Re(CO)_5$ (the former band has both Q and P branches visible). Just as in the Mn compound, ν_{22} is displaced *upward* upon deuteration, to 607.5 cm^{-1} in the gas phase, as $\rho(CD_3)$ comes in below at 585 cm^{-1}. The three A_1 skeletal stretching modes can be assigned by joint use of CD_3 and ^{13}C shifts, seen in both infrared and Raman solid phase spectra, to the frequencies 473, 455, and 450 cm^{-1} for the ^{12}C species. As shown by the calculations below, the lowest of these frequencies takes on more and more the character of ν(M–Me) with increase in the methyl mass. The middle frequency involves more axial than equatorial M–CO stretching. The two lower frequencies are significantly higher than their analogues in the Mn compound, and the highest is slightly lower.

The very strong solid-phase band at ~375 cm^{-1}, Figure 5, must arise from ν_{24}(E) (ν(M–CO^{eq})) and its displacement of 88 cm^{-1} below its Mn counterpart is of the order of magnitude to be expected from the change in mass of the metal atom, so that no force constant variation is necessarily involved.

Both the gas- and the solid-phase spectra suggest that a fundamental near 533 cm^{-1} moves down by about 10 cm^{-1} on deuteration, which identifies it as ν_{23}(E) (δ(MCO)). A smaller deuteration shift of about 3 cm^{-1} is exhibited by the weak solid-phase infrared band at 434 cm^{-1}, and this would have to be due to ν_{25}(E) (δ(MCO)). Its virtual coincidence with ν_{23} in the Mn compound at 440 cm^{-1} (solid) could be explained through the coupling arising from the crossing of ν_{24} from above (Mn) to below (Re). However, the fact that it derives from the F_{1g} mode ν_5 in $M(CO)_6$, which varies little with the nature of M, may also be relevant.

Three apparently isotope-independent frequencies near 533, 503, and 418 cm^{-1} then remain to be explained, the last of these being an exceedingly weak and dubious band in the infrared solid spectrum. The A_2 δ(MCO) mode ν_{10}, assigned at 374 cm^{-1} in the Mn compound, should not move appreciably, as argued above, and so should be obscured by the very strong band due to ν_{24}. A similar constancy is expected for the B_1 mode ν_{13}, so that if this occurs at ~609 cm^{-1} in the Mn compound,[3] it will also be obscured in the Re compound, this time by the intense bands due to ν_5 and ν_{22}. There is in fact a very weak sharp peak at 589 cm^{-1} in the infrared solid film spectrum of $^{13}CD_3Re(CO)_5$. For the B_2 mode ν_{16}, a depression rather less than that found in ν_5 and ν_{22} should occur, and this would be adequately fulfilled if ν_{16} is assigned at 533 cm^{-1}, displaced by about 25 cm^{-1} from the Mn band at 558 cm^{-1}. The remaining ν(MC) mode, $\nu_{14}(B_1)$, is assigned at 423 cm^{-1} in $MeMn(CO)_5$; there is no obvious reason for a dramatic rise in frequency from Mn to Re, so that the 418-cm^{-1} band in $MeRe(CO)_5$ appears to be a more acceptable candidate than the 503-cm^{-1} band. This leads to the tentative conclusion that the 503-cm^{-1} band must be a combination. The need for more data here is very apparent.

Tables II and V contain some possible assignments for nonfundamental bands. A difference band at 1869 cm^{-1} (Table II) moves upward on deuteration by 9 cm^{-1} and leads to a value of 129 cm^{-1} for ν_{26}(E). Another likely difference band at 1922 cm^{-1} suggests a fundamental at 76 cm^{-1}.

An A_1 Force Field. Since a general force field for even this small group of vibrations is far out of reach in a molecule of this size, we sought only the moe limited objective of comparing force fields for the Mn and Re compounds with identical constraints in the two cases. The symmetry coordinates are listed in Table VI and are conventional for this type of molecule.[19] Twelve interaction constants were constrained to values used in $BrMn(CO)_5$[4] and another, $F_{1,2}$ (ν_s(CH):$\delta_s(CH_3)$), was given a value of 0.15 mdyn $Å^{-1}$, comparable with those in methyl halide molecules.[20]

(18) However, there is an apparent shift of about 3 cm^{-1} in the shoulder at 571 cm^{-1} seen in the gas-phase $^{12}CH_3$ spectrum which, if genuine, suggests an A_1 or E symmetry. This might be connected with the apparent polarization character of the Raman line at 571 cm^{-1} in the solution spectrum.[3]

(19) The δ(CMC) coordinate δ_8 was defined with only one set of CMC angles, in contrast to the definition of δ_7 in ref 4. Only in this way could we obtain a $F_{8,8}$ for $MeMn(CO)_5$ similar to $F_{7,7}$ in $BrMn(CO)_5$[3].

(20) Duncan, J. L.; Allan, A.; McKean, D. C. *Mol. Phys.* **1970**, *18*, 289.

Table VI. A_1 Force Fields for $MeM(CO)_5$

Refined Constants

	Mn	Re		Mn	Re
$F_{1,1}$	4.871 (36)	4.812 (6)	$F_{4,6}$	0.053 (18)	0.032 (9)
$F_{2,2}$	0.460 (4)	0.472 (7)	$F_{5,5}$	16.38 (16)	16.10 (25)
$F_{2,3}$	−0.312 (5)	−0.301 (8)	$F_{6,6}$	2. 848 (8)	3.586 (17)
$F_{3,3}$	1.577 (13)	1.833 (8)	$F_{7,7}$	17.23 (23)	17.28 (37)
$F_{3,4}$	0.160 (11)	0.123 (7)	$F_{8,8}$	0.612 (31)	(0.75)
$F_{4,4}$	2.699 (23)	3.176 (12)	$F_{9,9}$	1.060 (11)	0.968 (17)

Constrained Constants (Both Molecules)[a]

$F_{1,2}$	0.15	$F_{4,5}$	0.758	$F_{4,7}$	−0.13	$F_{4,8}$	0.396	$F_{4,9}$	−0.097
$F_{5,7}$	0.408	$F_{5,8}$	0.02	$F_{5,9}$	−0.16	$F_{6,7}$	0.26	$F_{6,8}$	−0.22
$F_{7,8}$	0.07	$F_{8,9}$	0.026						

Symmetry Coordinates

$S_1 = \nu_s(CH_3)$; $S_2 = \delta_s(CH_3) = (\sum\angle HCH - \sum\angle HCM/\sqrt{6}$; $S_3 = \nu(M\text{–}Me)$;
$S_4 = \nu(M\text{–}CO^{ax})$; $S_5 = \nu(C\text{–}O^{ax})$; $S_6 = \nu(M\text{–}CO^{eq})$; $S_7 = \nu(C\text{–}O^{eq})$;
$S_8 = (\psi_1 + \psi_2 + \psi_3 + \psi_4)^b(\delta\ CMC))$; $S_9 = \delta(MCO)$

Geometry Assumed[c] (in Order Mn, Re)

$r_{C\text{–}H}$ = 1.0959, 1.0959 Å; ∠HCH = 109.471°; r(M–Me) = 2.185, 2.308 Å;
$r(M\text{–}CO^{ax})$ = 1.82, 2.00 Å; $r(M\text{–}CO^{eq})$ = 1.86, 2.00 Å; r(C–O) = 1.141, 1.13 Å;
$\angle C^{eq}MCO^{ax}$ = 94.7, 96.0°; $\angle MCO^{eq}$ = 177, 177°

[a] From $BrMn(CO)_5$, ref 4. [b] Angles defined in ref 4. See also text. [c] References 21 and 22.

Table VII lists the observed frequencies and frequency shifts used, together with their calculated values. The skeletal bending mode in $MeRe(CO)_5$ has not yet been observed and was set arbitrarily at 90 cm^{-1}, this assumption having no measurable effect on the stretching force constants. The only ^{13}C shift of high quality is on $\delta_s(CH_3)$ or $\delta_s(CD_3)$, leading to a well-defined value of $F_{2,3}$ ($\delta_s(CH_3)$:ν(M–CH_3)) in each molecule. The other, less accurate, shifts are quite well reproduced when two other interaction constants, $F_{3,4}$ and $F_{4,6}$, are allowed to refine.

The refinement problem is basically to find the correct solution for the interpretation of ν_6, ν_7, and ν_8, which lie close together in the range 400–490 cm^{-1}. Alternative solutions to the one tabulated were sought but not found. While in such a situation it is hard to be certain that one has refined to the correct force field, particularly when so many constants are constrained, the results make physical sense and there is no reason to believe that the absolute or relative values of the calculated force constants are grossly in error.

The values of $F_{8,8}$ suggest that the arbitrary frequency of 90 cm^{-1} for the skeletal bend in $MeRe(CO)_5$ is too high. It is comforting to find fairly similar values of $F_{3,4}$ for the two compounds. Whether the difference of 0.08 mdyn $Å^{-1}$ in the two quite small values of $F_{4,6}$ is real is uncertain.

The potential energy distributions for the vibrations ν_6, ν_7, and ν_8 are shown in Table VIII, listing only the skeletal stretching contributions. The results indicate the high degree of mixing of M–CH_3 and M–CO^{ax} stretching in the highest of the frequencies

Table VII. Observed and Calculated Frequencies for $MeM(CO)_5$, A_1 Species

	frequencies							
	M = Mn				M = Re			
	ν_{obsd}[a]	ν_{calcd}	$\Delta\nu_{obsd}$[a,e]	$\Delta\nu_{calcd}$[e]	ν_{obsd}[a]	ν_{calcd}	$\Delta\nu_{obsd}$[a,e]	$\Delta\nu_{calcd}$[e]
CH_3	2898 (20)[b]	2898.7		2.5	2879 (20)[b]	2881.1		2.5
	2116.5 (200)[b]	2116.5		0.0	2132.8 (20)[b]	2132.8		0.0
	2003.6 (200)[b]	2003.6		0.0	1997.6 (20)[b]	1997.6		0.0
	1191.1 (120)[b]	1196.2	5.1 (2)[b]	5.3	1212.0 (120)[b]	1216.0	5.7 (2)[b]	6.0
	668.0 (70)[b]	667.5		0.3	609.1 (60)[b]	608.4		0.1
	496.0 (50)[c]	495.5	3.5 (5)[c]	3.4	472.7 (10)[c]	471.8	5.2 (5)[c]	5.8
	420.0 (40)[c]	421.6	9.0 (10)[c]	9.0	454.5 (10)[c]	454.2	2.0 (5)[c]	2.0
	405.0 (10)[c]	405.8	0.0 (10)[c]	0.4	450.1 (10)[d]	448.3	6.1 (5)[d]	6.7
	100 (5)	100		0.3	90 (100)	(90)		0.1
CD_3		2116.5		0.0		2132.8		0.0
		2074.6		3.8		2062.3		3.9
		2003.5		0.0		1997.6		0.0
	903.1 (90)[b]	898.1	8.2 (2)	8.1	923.4 (90)[b]	918.9	9.3 (2)[b]	9.4
	666.9 (70)[b]	667.4		0.2	607.5 (70)[b]	608.4		0.0
	491.0 (50)[c]	491.4	2.0 (5)	1.9	464.0 (1)[c]	463.8	0.8 (5)[c]	0.8
	408.0 (10)[c]	407.1	0.0 (10)	0.6	451 (1)[c]	451.6	0.0 (5)[c]	0.2
	400.0 (41)[c]	400.8	8.0 (5)	7.4	425.6 (10)[d]	427.1	9.1 (5)[d]	10.0
	100 (10)	99.2		0.3		(90)		0.1

[a] In brackets, uncertainty used in refinement. No entry implies complete uncertainty. [b] Value in gas phase. [c] IR crystal spectrum at 78 K. [d] Raman crystal spectrum, room temperature. [e] $\Delta\nu = {}^{12}C\text{–}{}^{13}C$ shift.

Table VIII. PE Distributions for M–C Stretching Modes[a]

	$MeMn(CO)_5$				$MeRe(CO)_5$			
	ν_{calcd}	S_3 (M–CH_3)	S_4 (M–CO^{ax})	S_6 (M–CO^{eq})	ν_{calc}	S_3 (M–CH_3)	S_4 (M–CO^{ax})	S_6 (M–CO^{eq})
$^{12}CH_3$	495.5	0.45	0.65	0.02	471.8	0.69	0.35	0.08
$^{13}CH_3$	492.2	0.37	0.72	0.02	466.0	0.32	0.56	0.18
$^{12}CD_3$	491.4	0.32	0.75	0.02	463.8	0.14	0.64	0.25
$^{13}CD_3$	489.5	0.28	0.79	0.02	462.5	0.09	0.64	0.28
$^{12}CH_3$	421.6	0.65	0.28	0.05	454.2	0.21	0.02	0.73
$^{13}CH_3$	412.6	0.68	0.18	0.14	452.2	0.09	0.11	0.74
$^{12}CD_3$	407.1	0.13	0.00	0.82	451.6	0.03	0.22	0.64
$^{13}CD_3$	406.5	0.03	0.01	0.91	451.4	0.02	0.27	0.64
$^{12}CH_3$	405.8	0.01	0.07	0.87	448.3	0.20	0.60	0.12
$^{13}CH_3$	405.4	0.06	0.11	0.78	441.6	0.68	0.30	0.00
$^{12}CD_3$	400.8	0.61	0.25	0.10	427.1	0.87	0.11	0.00
$^{13}CD_3$	393.5	0.76	0.21	0.01	417.2	0.93	0.06	0.00

[a] $L_{ij}^2 F_{jj}/\lambda_l$.

Table IX. Stretching Force Constants (mdyn Å^{-1})

	C–H	M–CH_3	M–CO^{ax}	M–CO^{eq}		C–O^{ax}		C–O^{eq}			
	$f(\nu^{is})^a$	$f(A_1)$	$f(A_1)^b$	$f(A_1)$	$F(A_1)$	f(ef)	$f(A_1)$	f(ef)	F(ef)	f(c)	$F(A_1)$
$MeMn(CO)_5$	4.78	1.58	2.70	2.44	2.85	16.40	16.38	16.97	17.91		17.23
$MeRe(CO)_5$	4.71	1.83	3.18	3.18	3.59	16.27	16.10	17.05	18.22		17.28
$BrMn(CO)_5$[c]			2.62	2.09	2.50		16.79			17.88	18.14
$Cr(CO)_6$[d]			2.08				17.24				
$Mo(CO)_6$[d]			1.96				17.33				
$W(CO)_6$[d]			2.36				17.22				
$Ni(CO)_4$[e]			2.08				17.85				

[a] f = valence, F = symmetry force constant. ef = energy factored force field, A_1 = A_1 force field, c = complete force field. [b] Determined from $F_{6,6}$ assuming $(2f^c + f')(M–CO^{eq})(M–CO^{eq}) = 0.41$ as in $BrMn(CO)_5$, ref 4. [c] Reference 4. [d] Reference 5. Force constants are for complete force fields. [e] Reference 23. Force constants are for complete force field.

for the $^{12}CH_3$ species, with a gradual transfer of M–CH_3 motion into the lower frequencies as the mass of the methyl group increases. As expected, the coupling between the equatorial CO stretching and the other two stretching motions is much less extensive.

Stretching Force Constants: Chemical Significance. The calculated CH, MC, and CO stretching force constants in $MeMn(CO)_5$, $MeRe(CO)_5$, $BrMn(CO)_5$, and some binary metal carbonyls are listed in Table IX. In the A_1 force field the symmetry force constants $F_{3,3}$, $F_{4,4}$, and $F_{5,5}$ are identical with the valence force constants $f_{M–CH_3}$, $f_{M–CO^{ax}}$, and $f_{CO^{ax}}$, but $F_{6,6}$ and $F_{7,7}$ are not the same as $f_{M–CO^{eq}}$ and $f_{CO^{eq}}$. In order to convert these equatorial symmetry constants to the corresponding valence constants, we need to know the cis–cis and cis–trans equatorial interaction constants, which would only be available from a force field including the B_1 and E species vibrations. In the absence of this information we have obtained approximate values for $f_{M–CO^{eq}}$ by transferring the appropriate interaction constants from $BrMn(CO)_5$.[4] The valence constants $f_{CO^{eq}}$ are obtained from the energy-factored force field.

The CO stretching force constants derived from the A_1 and energy-factored force fields present a consistent picture of the relative CO bond strengths in the axial and equatorial ligands and in the manganese and rhenium compounds. The only significant numerical differences occur in the values of the symmetry constants $F_{CO^{eq}}$, which are 0.68–0.95 mdyn Å^{-1} higher in the energy-factored calculation. The discrepancies may be caused, at least in part, by the unavoidable constraints in the A_1 force field.

The trans effect of the non-π-bonding methyl ligand in increasing the population of the axial carbonyl π^* orbital is indicated by the low values of $f_{CO^{ax}}$ relative to $f_{CO^{eq}}$. In both force fields, the equatorial CO stretching constants are somewhat larger, and the axial constants smaller for $MeRe(CO)_5$ than for $MeMn(CO)_5$. The methyl trans effect, as measured by the difference $f_{CO^{eq}} - f_{CO^{ax}}$, thus appears to be rather stronger in the case of the rhenium compound. The trans effect of bromine in $BrMn(CO)_5$,[4] measured in the same way, is substantially greater than that of the methyl group, possibly because of a further repulsive interaction between the metal d_{xz} and d_{yz} orbitals and the lone-pair orbitals on the ligand atom.

The CO stretching force constants in the two methyl compounds are consistently smaller than the corresponding constants in $BrMn(CO)_5$. The values listed in Table IX to some extent underestimate this effect, as the force field calculations for $BrMn(CO)_5$ are based on solid-phase (KBr disc) frequency data,[4] whereas those for $MeMn(CO)_5$ and $MeRe(CO)_5$ use gas-phase frequencies. The more basic methyl ligand will increase electron density at the metal atom more effectively than bromide, thereby enhancing the tendency of the metal to transfer charge to the carbonyl π^* orbitals. This is essentially an electroneutrality effect initiated by the ligand → metal charge donation through the σ bond and affecting all the M–CO interactions; it is distinct from, and additional to, the specific π-trans effect of the ligand on the axial CO group, operating through the d_{xz} and d_{yz} orbitals.[24]

The values of $f_{M–CH_3}$ and f_{CH} in $MeMn(CO)_5$ and $MeRe(CO)_5$ illustrate the inverse relationship between metal–carbon and carbon–hydrogen bond strength which we have previously inferred from $\nu(CH^{is})$ and $D(M–CH_3)$ data. The MC stretching force constant $f_{M–CH_3}$ rises by 16% from $MeMn(CO)_5$ to $MeRe(CO)_5$, with a corresponding increase of 80%, from 29.4 ± 1.5 to 53.2 kcal mol^{-1}, in $D(M–CH_3)$;[25] at the same time, f_{CH} falls slightly, by about 1.5%, from Mn to Re, reflecting a downward shift of 20.4 cm^{-1} in $\nu(CH^{is})$.[2] The decrease in $\bar{D}$(C–H) is estimated to be about 1.7 kcal mol^{-1}, or 2%.

The metal–carbon bonds in $MeRe(CO)_5$ are markedly stronger than the corresponding bonds in $MeMn(CO)_5$, with $f_{M–CO^{ax}}$ and $f_{M–CO^{eq}}$ increasing by 18% and 30%, respectively, from Mn to Re, in addition to the increase, already mentioned, of 16% in $f_{M–CH_3}$. As the related CO stretching constants vary by less than 2%, it seems that the increase in bond strength from Mn to Re must be attributed primarily to an enhanced M–CO σ-bonding interaction. The stretching force constants for the axial and equatorial Re–CO bonds are accidentally equal (3.18 mdyn Å^{-1}), within the limits of uncertainty imposed by the force-field calculations. These are large values compared with the other M–CO stretching constants listed in Table IX and must represent particularly strong M–CO bonds. Similar trends in bond strength are observed in the adjoining group, in which the relative resistance to substitution of $W(CO)_6$, compared with $Cr(CO)_6$ or $Mo(CO)_6$, is attributed[26] to the increased metal–carbon σ-bond strength[5] in the tungsten compound.

The most striking feature of these results, however, lies in the information they provide on variations in the axial and equatorial M–CO bond strengths in $BrMn(CO)_5$, $MeMn(CO)_5$, and $MeRe(CO)_5$. In the bromo compound the axial constant $f_{M–CO^{ax}}$ is 0.53 mdyn Å^{-1} (25%) greater than $f_{M–CO^{eq}}$; in $MeMn(CO)_5$ the difference falls to 0.26 mdyn Å^{-1} (10%); and in $MeRe(CO)_5$ the axial and equatorial constants are equal. If we consider the trans effects of the bromide or methyl ligands only in terms of their influence on the axial M → CO π-system, then the result should always be to strengthen the axial M–CO bond relative to the equatorial bonds. This is of course precisely the effect indicated by the low values of $f_{CO^{ax}}$ relative to $f_{CO^{eq}}$. Moreover, as the π-trans effect of bromine, measured by the difference $f_{CO^{eq}} - f_{CO^{ax}}$, is clearly greater than that of methyl, we would expepect the difference between the axial and equatorial Mn–CO bond strengths to be larger in $BrMn(CO)_5$ than in $MeMn(CO)_5$, just as the experimental results indicate. Nevertheless, the variations in the relative M–CO bond strengths in the two molecules seem disproportionately large compared with the much smaller changes in the relative CO bond strengths. More importantly, the CO stretching force constants, as we have previously discussed, indicate that the π-trans

(21) Seip, H. M.; Seip, R. *Acta Chem. Scand.* **1970**, *24*, 3431.
(22) Rankin, D. W. H.; Robertson, A. *J. Organomet. Chem.* **1976**, *105*, 331.
(23) Jones, L. H.; McDowell, R. S.; Goldblatt, M. *J. Chem. Phys.* **1968**, *48*, 2663.

(24) Throughout this discussion, we assume that the highest occupied carbonyl σ-orbital is nonbonding, so that changes in the CO stretching force constants can be directly related to the CO π^* population. If the σ orbital is marginally antibonding, substitution of a trans ligand which weakens the M–CO σ bond will also very slightly weaken the CO bond, thereby enhancing its apparent trans effect through the π system. See, e.g.: Jones, L. H.; Swanson, B. *Acc. Chem. Res.* **1976**, *9*, 128.
(25) Lalage, D.; Brown, S.; Connor, J. A.; Skinner, H. A. *J. Organomet. Chem.* **1974**, *81*, 403.
(26) Dobson, G. R. *Acc. Chem. Res.* **1976**, *9*, 300.

effect of the methyl group in $MeRe(CO)_5$ is greater than it is in $MeMn(CO)_5$; thus if we pursue the argument purely in terms of the effect of the ligand on the axial M–CO π system we would expect the difference $f_{M-CO^{ax}} - f_{M-CO^{eq}}$ to be bigger in $MeRe(CO)_5$ than in $MeMn(CO)_5$ and certainly would not predict that the axial and equatorial Re–CO bonds would be equal in strength. We conclude that the overall trans effect of the methyl group must be considered in terms of a π effect, which strengthens the axial M–CO bond, and a σ effect, which weakens it. The very strongly σ-bonding methyl ligand will tend to monopolize the metal dz^2 orbital and will greatly reduce the ability of this orbital to accept electrons also from the axial carbonyl ligand. The much less basic bromide ligand, in contrast, will perturb the axial M ← CO σ interaction to a much lesser extent. Thus in $MeRe(CO)_5$ the σ and π effects are equal, or very nearly so, whereas in $MeMn(CO)_5$, which has an appreciably weaker metal–methyl bond than the rhenium compound, the π effect is becoming relatively more important and in $BrMn(CO)_5$ the π effect is predominant. An important point which must be repeated here is that these variations in axial and equatorial M–CO bond strengths are *not* reflected in the CO stretching force constants. If nothing else, our results demonstrate the limitations of trans effect series for metal carbonyl complexes derived only from CO stretching frequency measurements and empirical CO stretching force constant calculations.

Evidence from other sources to confirm the trends in M–CO bond strengths deduced from the force constant calculations would clearly be very desirable. Bond length measurements are an obvious possibility here, but it is necessary to bear in mind that in these multiply bonded systems very small changes in interatomic distances, which may be difficult to detect above normal experimental uncertainties, may reflect relatively large variations in bond strengths.

Theoretical (EHMO) calculations[27] of optimized geometries for $XMn(CO)_5$ molecules suggest that the group X has a negligible influence on the axial M–CO bond length; in all cases, however, including $MeMn(CO)_5$, the calculations make $M-CO^{ax}$ slightly shorter than $M-CO^{eq}$, by 0.03–0.04 Å. Experimental data are rather scanty. No structural information is available for $BrMn(CO)_5$, but in the related pentacarbonylmetal halides $ClMn(CO)_5$,[28] $ClRe(CO)_5$,[29] $BrRe(CO)_5$[30], and $IRe(CO)_5$[31] the axial M–CO bonds are consistently 0.05–0.10 Å shorter than the equatorial bonds. The difference between the two bond lengths in $HMn(CO)_5$ is smaller (0.02–0.03 Å), again in favor of a stronger axial bond.[32] Bond length data for $MeMn(CO)_5$[21] and $MeRe(CO)_5$[22] are available only from electron-diffraction experiments. The data here are not very sensitive to small changes in the axial M–CO distances,[22] and differences between the axial and equatorial M–CO bonds could not be distinguished in either case. In the former, the axial Mn–CO bond is assumed to be slightly shorter than the equatorial bond and in the latter the two Re–CO bond lengths are assumed equal. While these results are not conclusive, it seems clear that the differences between the axial and equatorial bond lengths in the two methyl compounds are very small and certainly must be much less than the differences of up to 0.10 Å reported for the pentacarbonylmetal halides. As far as they go, the experimental structural data are thus rather pleasingly consistent with the conclusions we have drawn from the vibrational study, although more extensive structural information and a complete force-field calculation are obviously desirable.

Conclusions

1. A_1 force-field calculations show that the metal–carbon (M–CO and $M-CH_3$) bonds in $MeRe(CO)_5$ are all stronger than the corresponding bonds in $MeMn(CO)_5$. There is an inverse relationship between the $M-CH_3$ and C–H bond strengths.

2. The trans effect of the methyl group consists of a π effect, which strengthens the axial M–CO bond, and a σ effect, which weakens it. In $MeRe(CO)_5$ the two effects are approximately equal and in $MeMn(CO)_5$ the π effect is rather more important.

3. Revised assignments are proposed for ν_{14} (B_1, $Mn-CO^{eq}$), 423 cm^{-1}, and ν_{10}, (A_2, $\delta(MnCO)$), 374 cm^{-1}, in $MeMn(CO)_5$.

4. The appearance of the $\rho(CH_3)$ absorption in $MeRe(CO)_5$ is interpreted in terms of a variation in the rocking force constant with internal rotation angle, together with free internal rotation. An anomalous gas–solid shift in $\rho(CH_3)$ in $MeMn(CO)_5$ may arise from the same source.

Acknowledgment. We thank S.E.R.C. for financial support (C.L., A.R.M., I.T.).

Supplementary Material Available: Tables of infrared and vibrational frequencies for $MeM(CO)_5$ and $MeRe(CO)_5$ species (4 pages). Ordering information is given on any current masthead page.

(27) Pensak, D. A.; McKinney, R. J. *Inorg. Chem.* **1979**, *18*, 3407.
(28) Greene, P. T.; Bryan, R. F. *J. Chem. Soc. A* **1971**, 1559.
(29) Cotton, F. A.; Daniels, L. M. *Acta Crystallogr.* **1983**, *C39*, 1495.
(30) Couldwell, M. C.; Simpson, J. *Cryst. Struct. Commun.* **1977**, *6*, 1.
(31) Russell, D. R.; Ruff, P. W., quoted in ref 29.
(32) La Placa, S. J.; Hamilton, W. C.; Ibers, J. A.; Davidson, A. *Inorg. Chem.* **1969**, *8*, 1928.